Inorganic Chemistry

Article

pubs.acs.org/IC

Coordination Chemistry of 6-Thioguanine Derivatives with Cobalt: Toward Formation of Electrical Conductive One-Dimensional Coordination Polymers

Pilar Amo-Ochoa,[†] Simone S. Alexandre,[‡] Samira Hribesh,[∥,⊥] Miguel A. Galindo,[∥] Oscar Castillo,[§] Carlos J. Gómez-García,[#] Andrew R. Pike,[∥] José M. Soler,[▽] Andrew Houlton,*[,∥] and Félix Zamora*[,†]

[†]Departamento de Química Inorgánica, Universidad Autónoma de Madrid, 28049 Madrid, Spain

[‡]Departamento de Física, UFMG, C.P. 702, 30123-970 Belo Horizonte, MG, Brazil

[§]Departamento de Química Inorgánica, Facultad de Ciencia y Tecnología, Universidad del País Vasco (UPV/EHU), Apartado 644, E-48080 Bilbao, Spain

[∥]Chemical Nanoscience Laboratory, School of Chemistry, Newcastle University, Newcastle upon Tyne NE1 7RU, United Kingdom

[⊥]Department of Chemistry, Faculty of Arts & Sciences, Al-Mergeb University, P. O. Box 40397/40414, Al-Khums, Libya

[#]Instituto de Ciencia Molecular, Universidad de Valencia, C/Catedrático José Beltrán, 2, 46980 Paterna, Valencia, Spain

[▽]Departamento de Física de la Materia Condensada, Universidad Autónoma de Madrid, 28049 Madrid, Spain

Supporting Information

ABSTRACT: In this work we have synthetized and characterized by X-ray diffraction five cobalt complexes with 6-thioguanine (6-ThioGH), 6-thioguanosine (6-ThioGuoH), or 2′-deoxy-6-thioguanosine (2′-d-6-ThioGuoH) ligands. In all cases, these ligands coordinate to cobalt *via* N7 and S6 forming a chelate ring. However, independently of reagents ratio, 6-ThioGH provided monodimensional cobalt(II) coordination polymers, in which the 6-ThioG$^-$ acts as bridging ligand. However, for 2′-d-6-ThioGuoH and 6-ThioGuoH, the structure directing effect of the sugar residue gives rise to mononuclear cobalt complexes which form extensive H-bond interactions to generate 3D supramolecular networks. Furthermore, with 2′-d-6-ThioGuoH the cobalt ion remains in the divalent state, whereas with 6-ThioGuoH oxidation occurs and Co(III) is found. The electrical and magnetic properties of the coordination polymers isolated have been studied and the results discussed with the aid of DFT calculations, in the context of molecular wires.

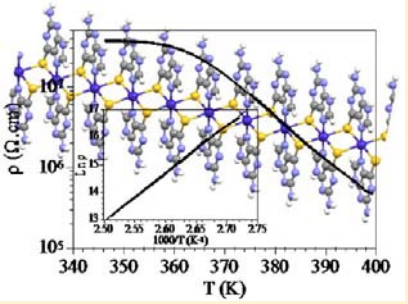

INTRODUCTION

Thiopurines are not naturally occurring nucleobases; however, these compounds and their ribose derivatives are some of the most active antimetabolites.[1] In addition, their pharmacology includes antitumor activity against certain tumors.[2] For instance, 6-mercaptopurine (6-MPH, Scheme 1) is one of the most widely used antileukemic agents and is used in essentially all modern acute lymphoblast leukemia treatment regimens,[3] while 6-thioguanine (Scheme 1) is useful in treating myelocytic leukemia.[4,5]

The interaction of this type of purine with metal ions has also attracted interest with initial studies primarily focused on understanding fundamental aspects of the coordination chemistry[6] and the possibility for developing new metal-containing drugs.[7] It has been found, for instance, that some metal complexes of purine derivatives such as 6-MP, especially those of platinum and palladium, show antitumor activity, which can be enhanced with respect to the activity of the free ligand.[8,9]

However, recent interest in potential applications of systems containing metal ions and nucleobases in the context of nanoelectronics based on DNA and related systems[10−15] prompted us to consider such compounds as promising candidates in the area of molecular materials. In particular, the 6-mercaptopurine systems have the capability for assembling metal ions, either as high nuclearity metal complexes[14,15] or, importantly, as 1D-coordination polymers, e.g., $[M(6\text{-MP})_2]_n$, which bear resemblance to the structure initially suggested for M-DNA.[16] Our first study focused on the one-dimensional coordination polymer $[Cd(6\text{-MP})_2]_n$ and demonstrated the isolation of single molecular chains of this polymer on a surface. While these were found to be insulating,[15] further DFT studies carried out on analogous $[M(6\text{-MP})_2]_n$ structures with a variety of transition metal ions revealed that substitution with Cu(II), Fe(II), Ni(II), or Co(II) should provide enhanced electrical conduction, on the basis of the smaller calculated HOMO−LUMO gap.[17] These studies prompted us to attempt the synthesis of various metal complexes and explore their electrical properties. We found that Ni(II) forms the expected $[Ni(6\text{-MP})_2]_n$ and $[Ni(6\text{-ThioG})_2]_n$ (6-ThioG = 6-thioguaninate) complexes as coordi-

Received: January 30, 2013
Published: April 18, 2013

   dx.doi.org/10.1021/ic400237h | *Inorg. Chem.* 2013, 52, 5290−5299

Scheme 1. Representation of the Artificial Nucleobases Used in This and Related Works: (a) 6-Mercaptopurine, (b) 6-Thioguanine, (c) 6-Thioguanosine, and (d) 2′-Deoxy-6-thioguanine

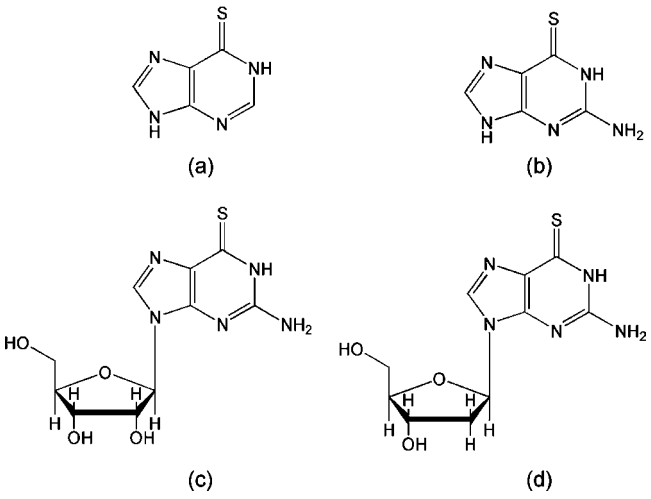

nation polymers and, in agreement with the theoretical predictions, exhibit semiconducting behavior.[12]

Cobalt, adjacent to Ni in the periodic table, presents interesting possibilities for inclusion in these thiopurine systems. As with Cd and Ni, Co is capable of adopting the necessary octahedral geometry for formation of the chainlike structure and may do so at two different levels of oxidation, viz., +2 and +3. Additionally, this introduces the possibility for magnetic effects, especially for d^7 Co(II). Materials integrating electrical and magnetic properties are of great interest in magnetic semiconductors, dilute magnetic semiconductors, and spintronic materials.[18,19] As our previous theoretical studies indicated that Co(II)-analogues of the 1D coordination polymers, based on these types of ligands, should have a significantly enhanced conductivity compared to Cd(II) derivatives,[17] it was therefore of interest to attempt to prepare and study such materials.

Here we report on the reactions of cobalt ions with a series of 6-thioguanine derivatives. We present 1-D coordination polymers based on Co(II), along with studies on their electrical properties. Additionally, we report the synthesis and characterization of Co(II) and Co(III) complexes of the corresponding 6-thioguanosine and 2′-deoxy-6-thioguanosine. These latter highlight two different forms in which the ligand can coordinate to the metal ions.

EXPERIMENTAL SECTION

Materials. All chemicals were of reagent grade and were used as commercially obtained. FTIR spectra (KBr pellets) were recorded on a Perkin-Elmer 1650 spectrophotometer. Elemental analyses were performed by the Microanalysis Service of the University Autónoma de Madrid on a LECO CHNS-932 microanalyzer. Thermal analyses (TG/DTA) were performed on a TA Instruments SDT 2960 thermal analyzer in a synthetic air atmosphere (79% N_2/21% O_2) with a heating rate of 5 °C min^{-1}.

Synthesis of $\{[Co(6\text{-ThioG})_2]\cdot 2H_2O\}_n$ (1). A mixture of $CoSO_4\cdot 7H_2O$ (150 mg, 0.533 mmol) and 6-thioguanine (160 mg, 0.960 mmol), in a buffer acetic acid/sodium acetate solution (8 mL, 0.1 M, pH 4.5), was stirred at room temperature for 10 min, sealed in a 23 mL Teflon-lined autoclave and heated at 160 °C for 72 h. Then, the autoclave was slowly cooled (0.3 °C/min.) to ambient temperature. The resulting pink-red crystals were washed with water and dried in air (140 mg, 63.6%, yield based on Co). Anal. Calcd (Found) for $C_{10}H_{12}N_{10}O_2S_2Co$: C, 28.11 (27.97) %; H, 2.83 (3.26) %; N, 32.78 (32.64) %; S, 15.01 (14.92) %. IR selected data (KBr, cm^{-1}): 3436 (bs), 3309(s), 3126(s), 2945(m), 1651(vs), 1628 (vs), 1580(s), 1501(s), 1364(s), 1312(m), 1253(m), 1201(m), 1144 (w), 1027(w), 965(w), 932(m), 857(m), 826(m), 640(m), 574 (m). The purity of the crystal samples has been checked by powder X-ray diffraction. The same compound is obtained employing thioguanine:cobalt ratio 3:1 or higher.

Synthesis of $\{[Co(6\text{-ThioG})_2]\}_n$ (2). Crystals of **2** were obtained upon heating compound **1** at 90 °C. Anal. Calcd (Found) for $C_{10}H_8N_{10}S_2Co$: C, 30.69 (30.51) %; H, 2.06 (2.03) %; N, 35.80 (35.93) %; S, 16.39 (16.22) %.

Synthesis of $[Co(2'\text{-d-6-ThioGuoH})_3](NO_3)_2\cdot 2H_2O$ (3). 2′-Deoxy-6-thioguanine (86.03 mg, 0.304 mmol) was dissolved in methanol (10 mL), and a solution of cobalt nitrate $Co(NO_3)_2\cdot 6H_2O$ (68 mg, 0.234 mmol) also in methanol (3 mL) was added. The mixture was refluxed, with stirring, at 60 °C overnight. After 24 h the solution was filtered and left to crystallize at room temperature by slow evaporation. After 5 days a crystalline precipitate was isolated by filtration (65 mg, 31% yield), from which a small green single crystal of **3** suitable for X-ray structure determination was obtained. Anal. Calcd (Found) for $C_{30}H_{44}N_{18}O_{20}S_3Co$: C, 31.83 (31.81); H, 3.92 (3.94); N, 22.27 (22.14). IR selected data (cm^{-1}): 3300 (w), 3200 (m), 2916 (m), 2845 (w), 1605 (s), 1375 (m), 1321(s), 1246 (m), 1202 (m), 1175 (m), 1092 (m), 1045 (w), 988 (m), 947 (m), 800 (m).723 (w), 603 (w). ES-MS: *m/z* (positive mode) 907.1469 (Calcd for $[Co(6\text{-MP})_3]^+$ 907.1471).

Synthesis of $[Co(6\text{-ThioGuo})_3]\cdot 1.5H_2O$ (4). 6-Thioguanosine (6-ThioGuoH) (74.4 mg, 0.248 mmol) was dissolved in mixture of water (10 mL) and methanol (10 mL), and then 10 mL of an aqueous solution of $Co(NO_3)_2\cdot 6H_2O$ (36.1 mg, 0.124 mmol) was added to the mixture. The mixture was refluxed and stirred at 86 °C for 3 h; after that, the pH of the solution was adjusted to 8 with NaOH and refluxed again for 3 h more. The solution was then filtered and kept at room temperature to afford 57 mg (48% yield) of dark green crystals suitable for X-ray structure determination. Anal. Calcd (Found) for $C_{30}H_{39}N_{15}O_{13.5}S_3Co\cdot 0.5NaOH$: C, 36.00 (36.59); H, 3.98 (3.22); N, 20.99 (19.96). IR selected data (cm^{-1}): 3248 (s), 3130 (s), 2972 (m), 2889 (s), 1591 (s), 1589 (s), 1371 (s), 1267 (s), 1192 (s), 1082(s), 982 (m), 935 (s), 873 (m), 630 (m). ES-MS: *m/z* (positive mode) 976.1069 (Calcd for $[Co(6\text{-MP})_3]Na^+$: 976.1060).

Synthesis of $[Co(6\text{-ThioGuo})(6\text{-ThioGuoH})_2](SO_4)\cdot 3H_2O$ (5). 2-Amino-6-mercaptopurine ribose (75 mg, 0.250 mmol) was dissolved in hot water (40 mL), and an aqueous solution (20 mL) of $CoSO_4\cdot 7H_2O$ (35 mg, 0.125 mmol) was added dropwise. After complete addition, the pH was adjusted to pH 8 using NaOH. The solution mixture was then refluxed for 3 h, allowed to reach room temperature, and filtered off through Celite. The clear solution stood at room temperature overnight, and crystals of the title compound were formed (20 mg, 15% yield) Anal. Calcd (Found) for $C_{30}H_{42}N_{15}O_{19}S_4Co$: C, 32.64 (32.36); N, 19.87 (20.08); H, 3.99 (4.05); S, 9.61 (9.57). IR selected data (cm^{-1}): 3104 (w), 1609 (vs), 1593 (vs), 1500 (m), 1464 (m), 1374 (s), 1276 (w), 1194 (s), 1085 (s), 1042 (m), 985 (w), 936 (s), 877 (w), 830 (w), 802 (w), 783 (s), 646 (m), 631 (m). ES-MS: *m/z* (positive mode) 955.1318 [Calcd for $Co(6\text{-ThioGuo})(6\text{-ThioGuoH})_2]^{2+}$: 955.1308].

The thermogravimetric analysis of compound **5** confirms the proposed formula. A first mass loss of 4.42%, taking place from room temperature up to 80 °C, is attributed to the release of the three crystallization water molecules (calcd 4.89%). The resulting anhydrous compound is stable up to 230 °C, after which it suffers several decomposition processes to lead Co_2O_3 above 540 °C (expt 7.67%, calcd 7.51%). The trivalent oxidation state of the metal center was confirmed by means of susceptibility measurements that showed the diamagnetic character of the compound. The absorption band at 1042 cm^{-1} in the IR spectra of compound **5** confirms the presence of SO_4^{2-} counterions.[20]

X-ray Data Collection and Structure Determination. Suitable crystals were mounted on glass fibers, and these samples were used for

dx.doi.org/10.1021/ic400237h | Inorg. Chem. 2013, 52, 5290−5299

Table 1. Single-Crystal Data and Structure Refinement Details for Compounds 1−5

	1	2	3	4	5
formula	$C_{10}H_{12}CoN_{10}O_2S_2$	$C_{10}H_8CoN_{10}S_2$	$C_{30}H_{43}CoN_{17}O_{17}S_3$	$C_{30}H_{39}CoN_{15}O_{13.5}0S_3$	$C_{30}H_{42}CoN_{15}O_{19}S_4$
weight (g mol^{-1})	425.33	391.31	1068.92	980.87	1103.96
cryst syst	triclinic	triclinic	trigonal	trigonal	trigonal
space group	$P\bar{1}$	$P\bar{1}$	$P3$	$P3$	$P3$
a (Å)	3.6653(3)	3.7380(4)	23.970(4)	18.815(5)	19.225(3)
b (Å)	9.6754(12)	9.3077(12)	23.970(4)	18.815(5)	19.225(3)
c (Å)	11.3399(11)	10.9407(11)	6.6297(11)	6.5787(18)	6.618(2)
α (deg)	110.236(10)	106.416(10)	90°	90°	90°
β (deg)	96.556(7)	99.161(8)	90°	90°	90°
γ (deg)	100.513(8)	99.614(10)	120°	120°	120°
V (Å^3)	364.08(6)	351.33(7)	3298.8(14)	2016.9(9)	2118.2(8)
Z	1	1	3	2	2
ρ_{calcd} (g cm^{-3})	1.940	1.850	1.614	1.615	1.731
μ (mm^{-1})	12.246	12.517	0.578	0.615	0.701
reflns collected	2275	2215	10941	19985	2771
unique data/params	1466/115	1419/106	6189/609	6695/378	2771/178
reflns $I \geq 2\sigma(I)$	1329	1203	5232	5233	1705
GOF (S)[a]	1.075	1.074	1.163	1.028	1.711
R1[b]/wR2[c] [$I \geq 2\sigma(I)$]	0.0408/0.1103	0.0463/0.1146	0.1022/0.2615	0.0557/0.1542	0.1769/0.4291
R1/wR2 (all data)	0.0460/0.1162	0.0571/0.1264	0.1166/0.2785	0.0717/0.1655	0.2203/0.4687

[a] $S = [\sum w(F_o^2 - F_c^2)^2/(N_{obs} - N_{param})]^{1/2}$. [b] $R1 = \sum||F_o| - |F_c||/\sum|F_o|$. [c] $wR2 = [\sum w(F_o^2 - F_c^2)^2/\sum wF_o^2]^{1/2}$; $w = 1/[\sigma^2(F_o^2) + (aP)^2 + bP]$ where $P = (\max(F_o^2, 0) + 2Fc^2)/3$ with a = 0.0683 (**1**), 0.0637 (**2**), 0.2000 (**3**), 0.1069 (**4**), 0.2000 (**5**), and b = 0.0759 (**1**).

Table 2. Selected Bond Lengths (Å) for Compounds 1−5

	1	2		3	4	5
Co1−N7	2.087(3)	2.088(3)	Co1−N7	2.067(8)	1.985(4)	1.96(3)
Co1−S6	2.5289(8)	2.5372(9)	Co1−S6	2.397(2)	2.3035(13)	2.287(9)
Co1−S6^{ia}	2.6416(8)	2.6676(10)	S6−C6	1.689(9)	1.733(4)	1.83(3)
Co1···Co1^{i}	3.6653(3)	3.7380(4)	Co2−N27	2.054(7)	1.998(4)	1.99(3)
S6−C6	1.748(3)	1.741(3)	Co2−S26	2.463(2)	2.3276(13)	2.282(10)
			S26−C26	1.664(9)	1.737(4)	1.69(3)
			Co3−N47	2.030(10)		
			Co3−S46	2.467(4)		
			S46−C46	1.724(12)		

[a] Symmetry codes: (i) $x + 1, y, z$.

data collection. The single crystal X-ray diffraction data were collected on a Agilent Technologies Supernova (**1**, 293(2) K, $\lambda_{Cu\ K\alpha}$ = 1.541 84 Å; **2**, 363(2) K, $\lambda_{Cu\ K\alpha}$ = 1.541 84 Å) and a Rigaku Saturn (**3** and **4**, 150 K, silicon double crystal monochromated synchrotron radiation: λ = 0.688 90 Å) diffractometers, and a Bruker SMART 1K CCD (**5**, 120(2) K, silicon[111]-monochromated synchrotron radiation: λ = 0.7020 Å). Information concerning data collection is summarized in Table 1. The structures were solved by direct methods using the SIR97 program (**1**, **2**, and **5**) and SHELXTL (**3** and **4**).[21] Full matrix least-squares refinements were performed on F^2 using SHELXL97.[22] All non-hydrogen atoms were refined anisotropically. The hydrogen atoms of the purine bases were either positioned geometrically and allowed to ride on their parent atoms, or located at the Fourier difference map and fixed at that position (hydroxyl and water O−H). Calculations were performed using the WinGX crystallographic software package or SHELXTL.[23]

In compound **5**, only very small specimens were obtained, and the low quality of the X-ray diffraction data only allowed a preliminary crystal structure solution. The ribose residue of the guanosine was refined using soft restraints on its C−C and C−O bond distances. The contribution of the missing solvent molecules and counterions was subtracted from the reflection data by the SQUEEZE method[24] as implemented in PLATON.[25] No attempt to localize the hydrogen atoms was performed. Only cobalt and sulfur atoms were refined anisotropically. Selected bond lengths and hydrogen bonding interactions are listed in Tables 2 and 3.

Conductivity Measurements. The dc electrical conductivity measurements were carried out with the four or two contacts methods (depending on the crystal size) on up to six single crystals of compound **1** in the temperature range 300−400 K since the resistance at room temperature exceeded the detection limit of our equipment ($5 \times 10^{11}\Omega$), precluding its study at low temperatures. The contacts were made with Pt wires (25 μm diameter) using graphite paste. The samples were measured in a Quantum Design PPMS-9 equipment. All the conductivity quoted values have been measured in the voltage range where the crystals are Ohmic conductors. All the measured crystals showed similar conductivity values and thermal behaviors. The cooling and warming rates were 0.5 and 1 K/min, and the results were similar in the cooling and warming scans.

Magnetic Measurements. Variable temperature susceptibility measurements were carried out in the temperature range 2−300 K with an applied magnetic field of 0.5 T on a ground polycrystalline sample of **1** (3.67 mg) with a SQUID magnetometer (Quantum Design MPMS-XL-5). The susceptibility data were corrected for the diamagnetic contributions of the sample as deduced by using Pascal's constant tables. The isothermal magnetization was measured in the same sample at 2 K with magnetic fields in the range 0−5 T.

Computational Methods. Our first-principles calculations were carried out using the linear combination of atomic orbitals (LCAO) method, implemented in the SIESTA code.[26,27] We employ two different exchange-correlation functionals: the nonlocal van der Waals density functional (vdWDF) of Dion et al.[28,29] as implemented in the

dx.doi.org/10.1021/ic400237h | Inorg. Chem. 2013, 52, 5290−5299

Table 3. Hydrogen Bonding Parameters (Å, deg) in Compounds 3 and 4

	H···A	D···A	D−H···A
Compound **3**			
N1−H···O2w	1.83	2.703(14)	170
N2−H···O61	2.08	2.926(16)	161
N2−H···O36^{i}[a]	2.00	2.832(12)	158
O16−H···O56^{ii}	1.98	2.813(16)	160
O17−H···O72^{iii}	2.02	2.841(14)	154
N21−H···O71	1.94	2.748(11)	153
N22−H···O57^{iv}	2.01	2.846(14)	158
N22−H···O71	2.19	2.946(13)	144
O36−H···O1w	2.06	2.825(19)	151
O37−H···O36^{iv}	1.84	2.637(12)	144
N41−H···O63	1.86	2.737(15)	178
N42−H···O62	2.01	2.865(16)	165
O56−H···N43	1.98	2.808(14)	174
O57−H···O1w^{v}	1.97	2.80(2)	167
O1w−H···O30	2.21	3.09(2)	150
O1w−H···O63^{vi}	2.59	3.38(4)	139
O2w−H···O16^{vii}	1.87	2.71(2)	162
O2w−H···O62	1.86	2.70(2)	158
Compound **4**			
N2−H···N21	2.12	2.976(5)	165
O16−H···O36^{i}	1.83	2.645(8)	160
O17−H···O37^{ii}	1.89	2.690(7)	162
O18−H···O38^{ii}	2.17	2.937(6)	141
N22−H···N1	2.19	3.047(5)	165
O36−H···N23	1.96	2.750(5)	160
O37−H···O1w^{iii}	1.76	2.615(11)	154
O38−H···O17^{iv}	2.07	2.850(8)	163
O1w−H···O1w^{v}	1.87	2.702(14)	154
O1w−H···O16^{vi}	1.85	2.670(12)	145

[a]Symmetry codes for compound **3**: (i) $-x + y + 2, -x + 2, z + 1$, (ii) $-y + 1, x - y, z + 2$, (iii) $-y + 1, x - y, z + 3$, (iv) $x, y, z + 1$, (v) $x, y, z - 1$, (vi) $-y + 2, x - y, z$, (vii) $-x + y + 1, -x + 1, z - 1$. Symmetry codes for compound **4**: (i) $-y + 1, x - y, z + 1$, (ii) $-x + y, -x, z + 2$, (iii) $x, y, z - 1$, (iv) $-y, x - y, z - 1$, (v) $-y + 1, x - y + 1, z$, (vi) $-x + y + 1, -x + 1, z - 1$.

SIESTA code[30] and the revPBE version of the generalized gradient approximation (GGA) in order to compare with our previous results in a similar system.[13] We use a basis of optimized double-ζ orbitals including polarization orbitals, and norm conserving pseudopotentials,[31] adding partial core corrections[32] for Co. The initial structures were obtained from the atomic coordinates determined by X-ray diffraction analysis of the crystal, and the geometries were optimized until the residual forces were less than 0.05 eV/Å.

RESULTS AND DISCUSSION

The coordination chemistry of thio-containing purine derivatives is quite well established,[6] in part due to the fact that some of these compounds present interesting biological activity. As ligands they offer a variety of binding sites for coordination to metal ions, with the S6 and/or the N7 being the preferred positions for binding. The coordination versatility of these compounds has allowed a wide range of different structural types of complex to be prepared.[6]

The reaction carried out between $CoSO_4$ and 6-thioguanine under solvothermal conditions (in a buffer acetic acid/sodium acetate) yields compound **1**, which consist of a 1D polymeric complex of formula $\{[Co(6\text{-ThioG})_2]\cdot 2H_2O\}_n$. This compound is isostructural with the previously reported Ni(II) derivative, and similar to some cadmium and nickel mercaptopurine analogues.[12,33] The crystal structure consists of parallel neutral chains of $[Co(6\text{-ThioG})_2]_n$ and crystallization water molecules which interact among them and with the hydrogen atoms of N2 and C8 of the 6-thioguaninato ligand by means of hydrogen bonding (Figure S1). The coordination polymer is based on stacked centrosymmetric $[Co(6\text{-ThioG})_2]$ entities, which are linked together through axial Co−S bonds, forming a linear chain along the crystallographic *a*-axis with an intrachain Co···Co distance of 3.665 Å. The deprotonated thioguanines act as bridging ligands, chelating one metal center through the N7 and S6 while also binding to a second cobalt atom from the adjacent entity also through S6. Two thioguanine bases chelated to the same metal center are parallel but not coplanar (interplanar distance 1.342 Å), probably as a result of steric hindrance between the S6 and C8(H). The stacking of the centrosymmetric $[Co(6\text{-ThioG})_2]$ entities produces parallel offset face-to-face aromatic interactions established between thioguanines on the same side of the chain. The overlap region involves the imidazolic ring and the pyrimidinic rings of adjacent purines (Figure 1). The geometrical parameters are in

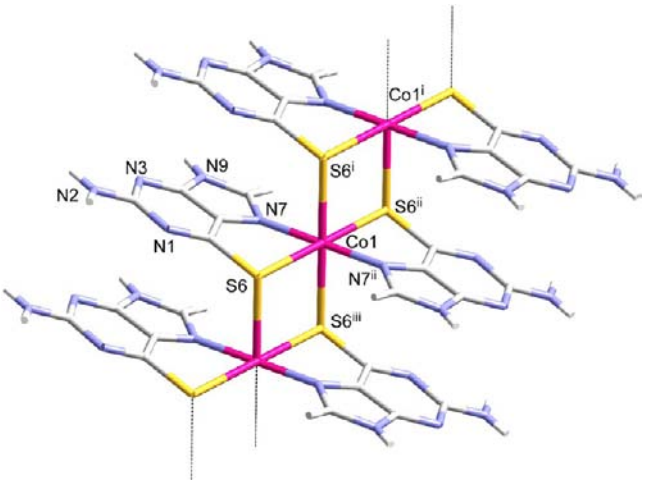

Figure 1. Fragment of the polymeric chain in compound **1** showing the labeling scheme.

the typical ranges for this type of noncovalent interactions (centroid···centroid distance = 3.277(4) Å; dihedral angle between rings = 2.5(3)°; lateral offset = 0.84 Å).[34]

The overall cohesiveness of the crystal structure is ensured by means of hydrogen bonding interactions that each polymeric chain establishes with four adjacent chains. The hydrogen bond interactions take place between the 6-thioguaninate ligands of different chains both through the Watson−Crick edge (N2(H)···N1: 3.009(8) Å) and through the Hoogsteen face (N9(H)···N3: 2.871(7) Å). The packing of the chains gives rise to channels parallel to the crystallographic *a* axis (representing 12.4% of the unit cell volume with *ca.* 6.2 × 6.3 Å^2 dimensions) that are occupied by crystallization water molecules that, based on the presence of short donor···acceptor atom distances, seem to be tightly hydrogen bonded among themselves (O1w···O1w: 2.935 and 3.225 Å) and to the metallo-polymer chains (N2(H)···O1w: 3.169 Å; C8(H)···O1w: 3.303 Å) (Figure S1). The supramolecular interactions between the water molecules and complex polymeric chains although not imperative for the cohesion of the crystal structure (compound **2** is a evidence of that)

dx.doi.org/10.1021/ic400237h | Inorg. Chem. 2013, 52, 5290−5299

reinforce the complementary hydrogen bonds established between thioguanines belonging to adjacent chains and therefore contribute to the robustness of the crystal structure. At the same time it exerts a subtle influence on the Co···Co distance as will be discussed later.

The magnetic properties of compound **1** confirm the presence of high spin Co(II) ions with a room temperature $\chi_m T$ value of *ca.* 2.6 cm^3 K mol^{-1}, which lies in the normal range (2.4−3.2 cm^3 K mol^{-1}) observed for high spin Co(II) octahedral complexes and higher than the expected value for an $S = {}^3/_2$ spin ground state, because of the orbital contribution arising from the ground $^4T_{1g}$ term.[35−37] When the temperature is lowered, the $\chi_m T$ product shows a continuous decrease to reaching a value of *ca.* 0.15 cm^3 K mol^{-1} at 2 K (Figure 3). This behavior indicates the presence of weak antiferromagnetic interactions in compound **1** (note that although isolated paramagnetic Co(II) complexes also show a decrease of the $\chi_m T$ product with decreasing temperatures, due to the spin−orbit coupling, this decrease is smoother and does not lead to values as low as 0.15 cm^3 K mol^{-1}).[35−37] The weak antiferromagnetic interaction is confirmed by the presence of a rounded maximum at *ca.* 5 K in the χ_m versus T plot (inset in Figure 2). This weak antiferromagnetic coupling can be

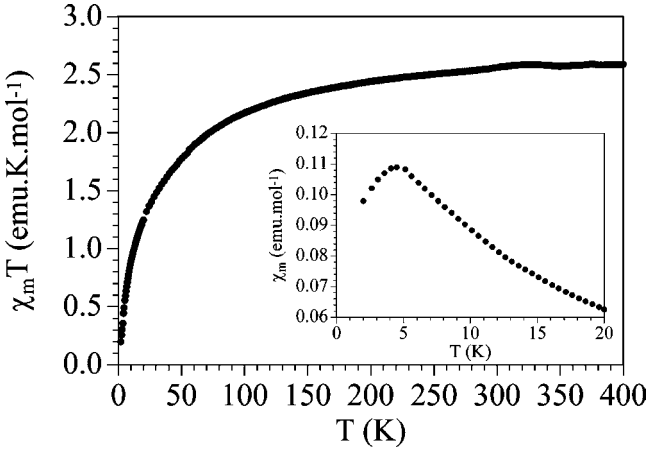

Figure 2. Thermal variation of the $\chi_m T$ product for compound **1**.

attributed to the presence of double thio-bridges connecting the Co(II) ions along the chain with relatively long Co−S bond distances of 2.5289(8) and 2.6416(8) Å.

On heating **1**, the water molecules of crystallization are released while the crystals remain intact, producing compound **2**. Hence, the crystal structure of **2** retains the 1D polymeric nature of the $[Co(6\text{-ThioG})_2]_n$ chains and the associated supramolecular interaction between the chains (Figure 3). However, the unit cell suffers a small shrinkage in volume of 12.8 $Å^3$. This is the common behavior when solvent of crystallization is removed, but what is more unusual is that this shrinkage takes place with an *elongation* in the propagation direction of the polymeric complex, in this case that of the crystallographic *a*-axis. This produces a slight lengthening of the Co···Co distance within the chain (0.073 Å), together with an increase in the Co−S−Co bond angles of *ca.* 2% (from 90.26(2)° to 91.77(3)°) and in the average Co−S bond distances of *ca.* 1% (from 2.5853(8) Å to 2.6024(10) Å). These three changes are expected to decrease the orbital overlap and, hence, the electron delocalization and the electrical conductivity when passing from compound **1** to **2**.

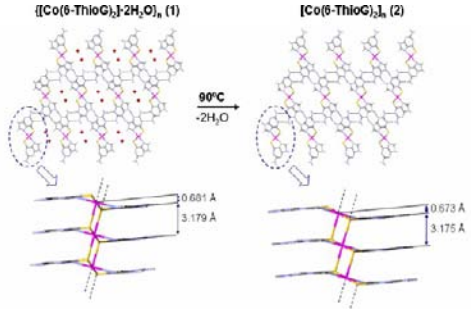

Figure 3. Crystal packing of compounds **1** and **2** viewed along the crystallographic *a* axis. Dotted lines represent hydrogen bonds.

An initial DFT calculation carried out on the analogous $[Co(6\text{-MP})_2]_n$ polymer (6-MP = 6-mercaptopurinato) gave a HOMO−LUMO gap of 0.78 eV,[13] a value 0.1 eV higher than that calculated for the corresponding Ni(II) analogue. However, as we reported, for Ni(II) coordination polymers the 6-ThioG derivative shows conductivity values 2 orders of magnitude higher than the 6-MP analogue,[12] and hence electrical measurements of **1** were of interest.

The dc electrical conductivity measurements of six crystals of compound **1** found very low room temperature conductivity values *ca.* 10^{-11} to 10^{-12} S cm^{-1} and semiconducting behavior, with activation energies in the range 1.4−1.6 eV (Figure 4). As

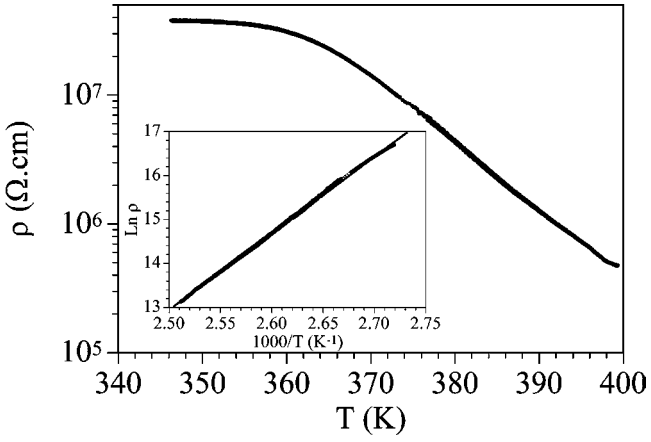

Figure 4. Thermal variation of the dc electrical conductivity of compound **1**. Inset shows the Arrhenius plot.

expected for semiconducting materials, at higher temperature (400 K) the conductivity is notably higher with values in the range 10^{-6} to 10^{-7} S cm^{-1}. All the attempts to measure the electrical conductivity of crystals of compound **2** lead to lower conductivity values, below our detection limit. As already mentioned, a possible reason explaining this difference may be the lengthening of the Co···Co distance, the Co−S−Co bond angles, and the Co−S bond lengths.

In order to understand the physical measurements, we computed the DFT electronic structure of $\{[Co(6\text{-ThioG})_2]\cdot 2H_2O\}_n$ as isolated chains as well as packed using the experimental X-ray lattice parameters, but allowing the atomic coordinates to relax (Supporting Information for additional information). Calculations were made with the vdW functional in order to ensure that the interactions between the polymer chains were well described in the calculation of the electronic structure of the crystal. We repeated the calculations using the

dx.doi.org/10.1021/ic400237h | Inorg. Chem. 2013, 52, 5290−5299

GGA functional to compare the results with those with the vdW-functional and with the band structure of $[Co(6\text{-}MP)_2]_n$ presented in our previous work.[13] The band structures we obtain with the two exchange-correlation functionals are quantitatively very similar for $\{[Co(6\text{-}ThioG)_2]\cdot 2H_2O\}_n$ in both the crystal and the isolated chain. We also computed the anhydrous $[Co(6\text{-}ThioG)_2]_n$ form to verify the effect of the water molecules on the conducting properties of the system. Analysis of the density of states (DOS) of both polymers indicates that the water molecules do not alter the electronic structure to any appreciable extent within an interval of ± ~1.0 eV of the HOMO−LUMO region, as shown in Figure 5.

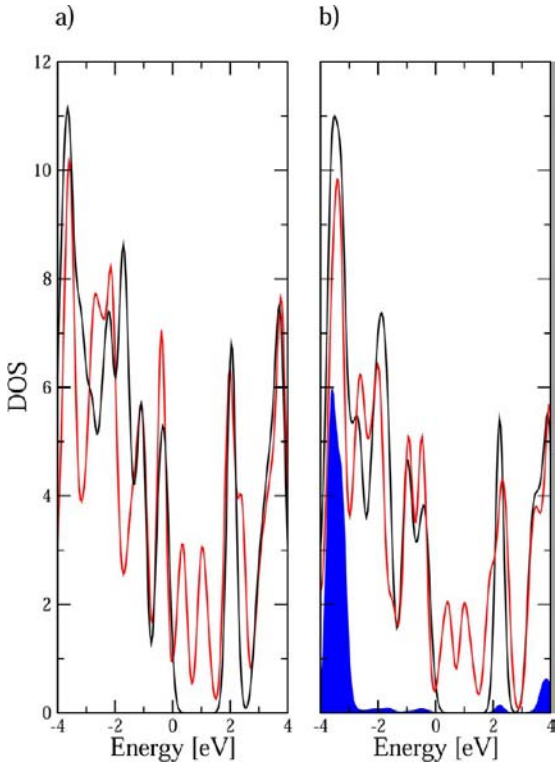

Figure 5. Density of states of $[Co(6\text{-}ThioG)_2]_n$ (a) and $\{[Co(6\text{-}ThioG)_2]\cdot 2H_2O\}_n$ (b). Red and black lines correspond to majority and minority spin states, respectively. Shaded blue curve shows the projected DOS on the water molecules. The Fermi level is at the zero of the energy scale.

Finally, we have also investigated the electronic structure of $\{[Co(6\text{-}ThioG)_2]\cdot OH\cdot H_2O\}_n$. This was to further explore the possible role of the water-derived species present in the crystal lattice. The substitution of one water molecule by an OH^- anion simulates charge doping, and generates holes in the valence band. The calculated energy gap values suggest that the antiferromagnetic ground state is the most reasonable one since it gives a much higher energy gap (even if it is still below the experimental one). The ferromagnetic ground state gives a too low energy gap. Furthermore, the antiferromagnetic ground state agrees with the experimental one found with the SQUID measurements. The difference between the energy gap obtained from the calculations and the experimental data may simply be attributed to crystal defects, mainly Co(II) vacancies in the chain leading to a charge localization of the charge since the delocalization is hindered. The effect is an increase in the resistivity and in the activation energy.

DFT calculations also provided details of the compounds magnetic structure, and we have obtained degenerate antiferromagnetic and ferromagnetic ground states in $\{[Co(6\text{-}ThioG)_2]\cdot 2H_2O\}_n$, with magnetic moments of 3.0 μB per Co atom. These magnetic ground states differ from the magnetic moment of 1.0 μB per Co atom that we found previously for a system with a structure based on the $[Co(6\text{-}MP)_2]_n$ framework.[13] Figure 6 shows the band structures of the

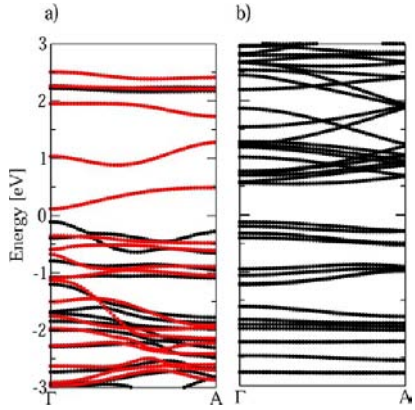

Figure 6. Band structures of $\{[Co(6\text{-}ThioG)_2]\cdot 2H_2O\}_n$ in (a) ferromagnetic solution, red and black lines correspond to majority and minority spin states, respectively; and (b) antiferromagnetic solution, the Fermi level is at the zero of the energy scale.

ferromagnetic and antiferromagnetic solutions for $\{[Co(6\text{-}ThioG)_2]\cdot 2H_2O\}_n$. Note that although the calculations indicate that the ferro- and antiferromagnetic ground states are degenerate, the presence of crystal defects and vacancies (as suggested by the dc conductivity measurements, see below) leads to a slight lowering of antiferromagnetic state, to become the ground state. This is in agreement with the SQUID measurements, that show the presence of a very weak antiferromagnetic coupling.

In an effort to prepare nucleoside analogues of **1**, a number of reactions with either 6-thioguanosine (6-ThioGuoH) or 2′-deoxy-6-thioguanosine (2′-d-6-ThioGuoH) and Co(II) ions were explored. We have been able to isolate and crystallographically characterize compounds from the following reactions: (i) 2′-d-6-TGH with $Co(NO_3)_2$ in refluxing MeOH yielded green crystals of compound $[Co^{II}(2'\text{-}d6\text{-}ThioGuoH)_3](NO_3)_2\cdot 2H_2O$ (**3**), (ii) 6-ThioGuoH with $Co(NO_3)_2$ in a refluxing 1:1 H_2O:MeOH mixture adjusted to pH 8 that yielded dark green crystals of compound $[Co^{III}(6\text{-}ThioGuo)_3]\cdot 1.5H_2O$ (**4**), and (iii) 6-ThioGuoH with $CoSO_4$ in aqueous solution at pH 8 that yielded, after recrystallization, compound $[Co^{II}(6\text{-}ThioGuo)(6\text{-}ThioGuoH)_2](SO_4)\cdot 3H_2O$ (**5**). Compounds **3**−**5** contain discrete octahedral complexes with the cobalt atom lying on a 3-fold rotation axis. The molecular structures of these complexes are shown in Figures 7−9. In each compound, three thio-nucleoside ligands chelate the metal center through the S6 and N7 donor atoms, giving rise to the same five-membered chelate rings present in **1** and **2**. The coordination sphere of the metal center corresponds to a chiral, trigonally elongated, *fac*-N_3S_3 octahedral environment. Variations in the metal ion oxidation state and the protonation state of the ligand (Figure 10) in all three instances were observed and are discussed in the following descriptions of the unique structures of **3**, **4**, and **5**.

dx.doi.org/10.1021/ic400237h | Inorg. Chem. 2013, 52, 5290−5299

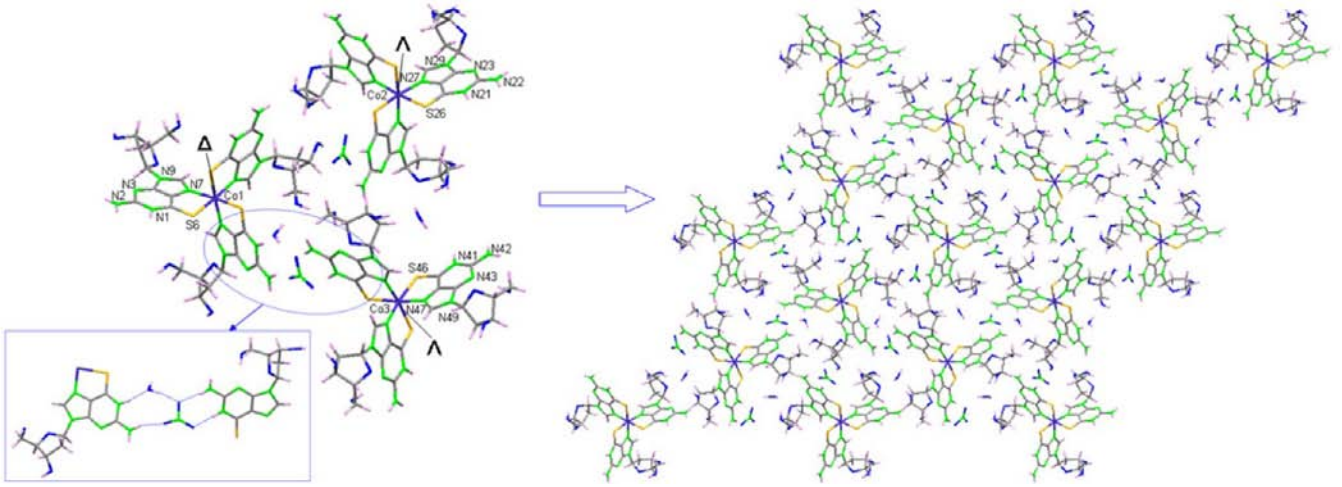

Figure 7. Crystal packing of $[Co(2'\text{-d-6-ThioGuoH})_3]^{2+}$ entities showing the supramolecular interactions in compound **3**.

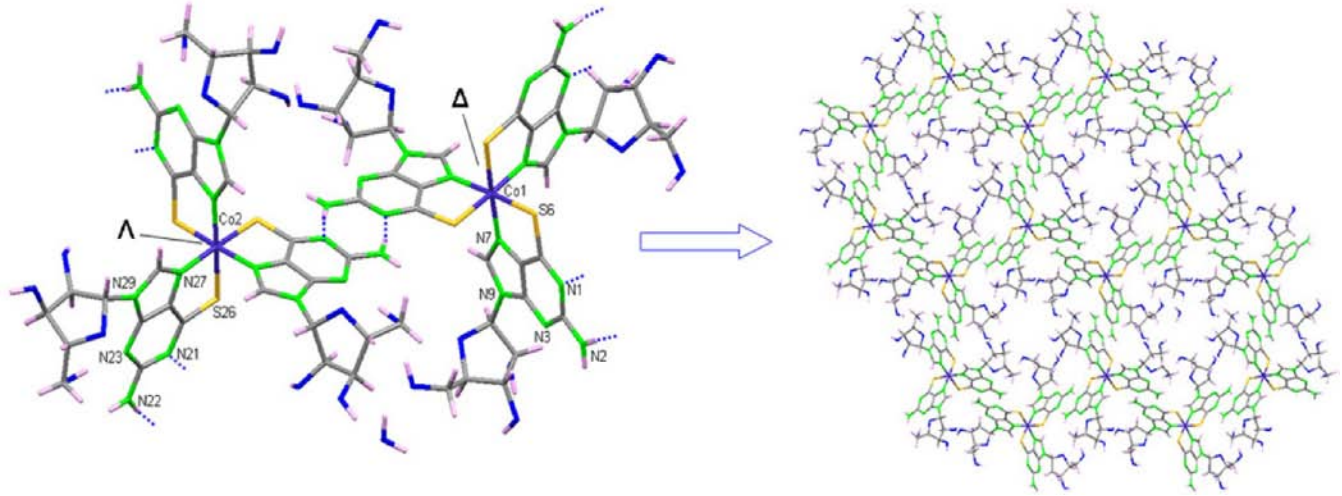

Figure 8. Supramolecular assembly of $[Co(6\text{-ThioGuo})_3]$ entities in compound **4** showing the presence of 1D channels running along the *c* axis. The crystallization water molecules placed inside the channels have been omitted for clarity.

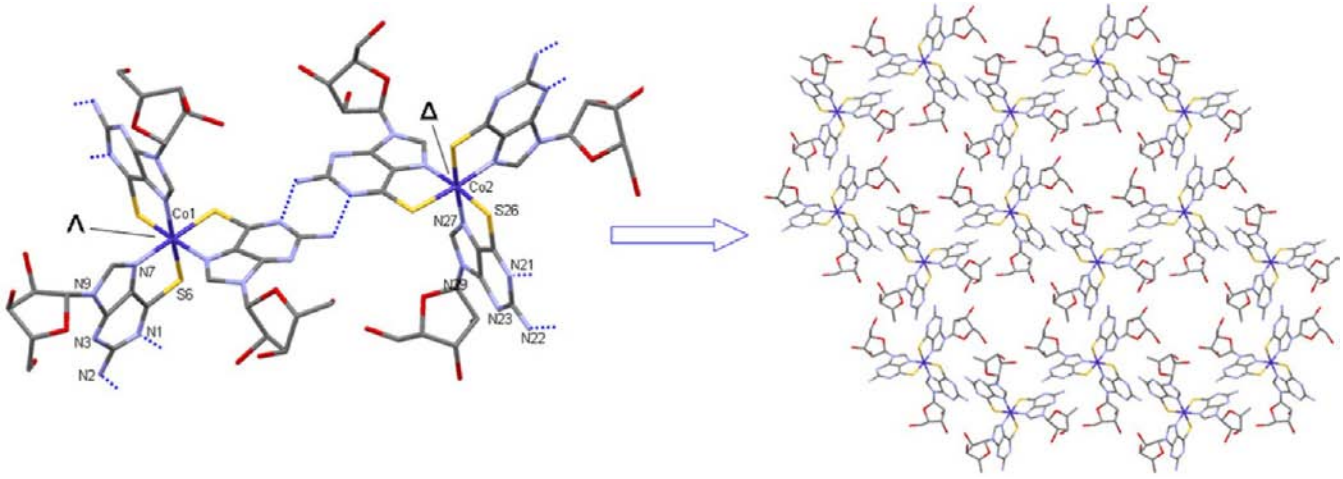

Figure 9. Crystal structure of compound **5** showing the presence of 1D channels running along the *c* axis. The sulfate counterions and water molecules placed inside the channels have been omitted for clarity. Dashed lines indicate hydrogen bonds.

In an attempt to synthesize a coordination polymer between Co(II) and 2′-d-6-ThioGuoH, the ratio of metal to ligand used in the synthesis of the previously reported Cd(II)/6-mecaptopurine system was followed.[14] This resulted in a single crystal of **3**, $[Co(2'\text{-d-6-ThioGuoH})_3](NO_3)_2{\cdot}2H_2O$, suitable for X-ray analysis, and no further attempts to control the

dx.doi.org/10.1021/ic400237h | *Inorg. Chem.* 2013, 52, 5290−5299

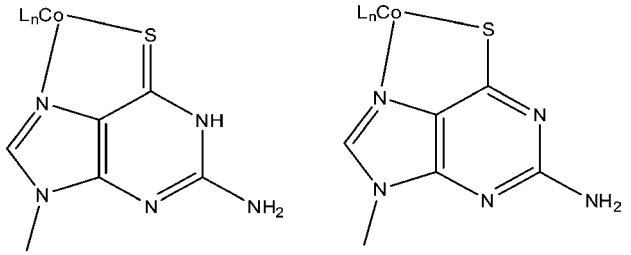

Figure 10. Formal representations of the thione (left) and thiol (right) forms of 6-thioguanine found in **4** and **5**, respectively.

reactant ratio were made. Compound **3** contains three independent molecules in the unit cell: two Λ isomers and one Δ isomer. The Co−S bond lengths range from 2.397(3) to 2.469(5) Å while the Co−N distances span 2.035(12)−2.065(10) Å. The metal ion oxidation state is Co(II), charge balanced by two nitrate anions in the crystal lattice, with the coordinating 2′-d-6-ThioGuoH being in the neutral, formally thione, form in contrast to the anionic form in **1** and **2** (Figure 10). Concomitant with this fact is the shorter average C═S bond length (C═S range = 1.662(10)−1.723(14); C═S_{Av} = 1.688 Å) compared to that found in **4** (*vide infra*).

In compound **4**, $[Co(6\text{-ThioGuo})_3]\cdot 1.5H_2O$, two independent molecules are found in the unit cell. Here, the 6-thioguanosine ligands are deprotonated at N(1), in keeping with the basic pH of the reaction, and can be considered as the anionic thiol form, 6-TG^- (Figure 10). In line with this is the expected increase in the C6−S6 bond lengths (in the range 1.733(4)−1.742(4) Å with an average value of 1.738 Å), compared to the thione form in **3** and **5** (*vide infra*). As there is no other anion in the crystal structure, the oxidation state of the metal center corresponds to Co(III). This increase in oxidation state is reflected in the slight decrease in the metal−ligand bond lengths, *viz*., Co−S = 2.3039(13)−2.3266(13), Co−S_{Av} = 2.315 Å; Co−N = 1.985(4)−1.996(4), Co−N_{Av}= 1.991 Å, compared to **3**. Room temperature magnetic susceptibility measurement indicates the diamagnetic nature of compound **4**, consistent with an octahedral low-spin d^6 configuration.

A previous study[33] has shown that the major structural effect of N(1) protonation/deprotonation is an increase in the C(6)−N(1)−C(2) angle in the former case. In keeping with this, the C(6)−N(1)−C(2) angles in compound **3** (119.0(10)−123.6(7)°) are larger than in **4** (117.1(3)−117.3(3)°). Moreover, the C(6)−N(1) bond length of the protonated ligands in **3** is longer, range 1.358(13)−1.388(13) Å, compared to the deprotonated form in **4** (1.321(6)−1.328(6) Å). This again is consistent with the assignment of the two tautomeric forms in the respective complexes, thione in **3** and the thiol-form in **4** (Figure 10), and illustrates the ability of the ligand to coordinate well to either oxidation state of the metal.

The X-ray analysis of **5** with formula $[Co(6\text{-ThioGuo})(6\text{-ThioGuoH})_2](SO_4)\cdot 3H_2O$ is of poor quality, but is included here as it illustrates the possibility of complex formation with inequivalent forms of coordinated nucleoside (Figure 10). As in **1** and **2**, the 6-thioguanosinate ligand is bound to the metal center through S6 and N7 donor positions, and these generate a trigonally elongated *fac*-N_3S_3 octahedral environment. Two crystallographic independent complexes, with opposite chilarity, Δ and Λ, are found in the unit cell, with metal−ligand bond lengths in the expected range (Co−S = 2.282(10)−2.287(9) Å; Co−N7 = 1.96(3)−1.99(3) Å). Although the X-ray diffraction data was of low quality, the C−S distances of 1.69(3) and 1.83(3) Å indicate the presence of both neutral (thione isomer) and deprotonated (anionic thiol isomer) guanosine, in agreement with the proposed formula.

While none of these nucleoside-containing compounds feature the coordination polymer chain seen in **1** and **2**, there are some noteworthy aspects of the crystal packing of **3**−**5**. In **4** and **5** the monomeric entities are held together by means of complementary hydrogen bonds. Symmetry-related N2-(H)···N1 (3.019(17) Å) interactions between two adjacent ligands give rise to $R_2^2(8)$ ring formations[38−40] which afford 2D supramolecular sheets of Δ/Λ $[Co(6\text{-ThioGuo})_3]$. Additional hydrogen bonding interactions, involving the hydroxyl groups of these sugar residues, hold the layers together to generate the overall 3D supramolecular structure in which 1D channels extend along the crystallographic *c* axis. Crystallization water molecules occupy these channels establishing strong hydrogen bonding interactions with the ribose. The ribose group of the coordinated thioguanosine molecules presents a hydrophilic rim to the channel in which the water molecules (**4**) (Figure 11) and sulfate counterions (**5**) are located. Discussion of water

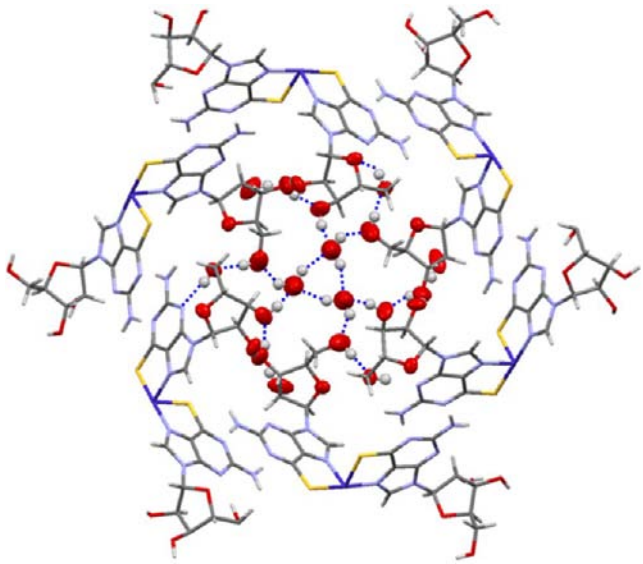

Figure 11. Hydrophilic nature of the 1D channels found in compound **4**.

aggregates or substructures in coordination compounds are of contemporary interest. The water molecules in these aggregates can adopt a great variety of arrangements.[41−50]

Although the crystal structure of compound **5** did not allow the location of hydrogen atoms, the similarities of the unit cell parameters and the hydrogen bonding donor−acceptor distances with those of compound **4** would indicate a similar supramolecular architecture. In **4** the channels have approximate dimensions 7.6 × 6.1 $Å^2$ representing 7.1% of the unit cell volume. The equivalent value for **5** indicates a larger, 9.3 × 9.3 $Å^2$, channel occupying 16% of the unit cell volume. This expansion to the unit cell is likely due to the inclusion of SO_4^{2-} counterions.

In **3**, the monomeric entities do not establish direct hydrogen interactions between the thioguanines. Instead, they are connected by means of hydrogen bonding interactions mediated by a nitrate anion and a water molecule. The nitrate anion interacts with the N6(H)/N1(H) face of a guanine to establish an $R_2^2(8)$ ring, with N6(H) of a second thioguanine

dx.doi.org/10.1021/ic400237h | *Inorg. Chem.* 2013, 52, 5290−5299

and a crystallization water molecule forming an $R_3^3(10)$ ring. Apart from these interactions the hydrogen bonding capability of the hydroxyl groups of the deoxyribose provides further connectivity throughout the crystal structure leading to a 3D network that does not feature channels as seen in compounds **4** and **5**.

At this point it is worthwhile to discuss the different nature of the complexes formed in the structures reported here. The thioguanine-containing compounds produce crystal structures composed of infinite $[Co(thioguaninate)_2]$ chains, while those based on thioguanosine show discrete *tris*-complexes. This latter stoichiometry is found despite not using a 3:1 ligand/metal ratio in the reactions. This finding suggests the sugar residue exhibits some structure directing effect on complex formation. The steric hindrance from this group would hinder the parallel stacking of the planar $[Co(thioguaninate)_2]$ units that completes the octahedral surrounding around the cobalt atom leading to chain formation, as seen in **1** and **2**. Instead, coordination of a third thioguanosine, to complete the coordination sphere, is favored.

In summary, the compounds reported here add to the rather limited number of complexes based on thioguanine derivatives. A search of the CSD shows only three records for M = Ni(II), Ir(III), and Co(III), although in the Ir(III) and Co(III) cases other coligands are present.[12] Moreover, a recent review[53] shows that the number of oligomeric and polymeric nucleobase-coordination compounds is limited compared to mononuclear species. Therefore, compounds **1** and **2** represent examples of the particularly small group of metal-containing 6-thioguanine complexes which show extended bonding motifs. On the other hand, the supramolecular crystal structure of compounds **4** and **5** continues a recently developed route for the generation of porous materials based on the use of complementary hydrogen bonding between nucleobases linked to discrete coordination entities.[54]

■ ASSOCIATED CONTENT

Supporting Information

Additional figures, tables, and details. X-ray crystallographic files in CIF format for compounds **1**−**5** (CCDC 921187−921191). This material is available free of charge via the Internet at http://pubs.acs.org.

■ AUTHOR INFORMATION

Corresponding Author

*E-mail: felix.zamora@uam.es (F.Z.).

Notes

The authors declare no competing financial interest.

■ ACKNOWLEDGMENTS

We acknowledge financial support from the Spanish Ministerio de Economía y Competitividad (MAT2010-20843-C02-01, MAT2008-05690/MAT, CTQ-2011-26507, FIS2009-12721, FIS2012-37549 and ACI2009-0969), Comunidad de Madrid (CAM 09-S2009_MAT-1467), Gobierno Vasco (IT-280-07), Generalitat Valenciana (Programs Prometeo 2009/95 and ISIC), and EU (FP6-029192), as well as Becas Fundación Caja Madrid de Movilidad para Profesores de universidades públicas. We thank Prof. L. Seijo for useful discussions.

■ REFERENCES

(1) Elion, G. B. *In Vitro Cell. Dev. Biol.* **1989**, *25*, 321.
(2) Elion, G. B. *Angew. Chem., Int. Ed.* **1989**, *28*, 870.
(3) Evans, W. E.; Relling, M. V. *Science* **1999**, *286*, 487.
(4) Freund, M.; Poliwoda, H.; Bodenstein, H.; Eisert, R. *Onkologie* **1985**, *8*, 150.
(5) Wiernik, P. H.; Glidewell, O. J.; Hoagland, H. C.; Brunner, K. W.; Spurr, C. L.; Cuttner, J.; Silver, R. T.; Carey, R. W.; Delduca, V.; Kung, F. H.; Holland, J. F. *Med. Pediatr. Oncol.* **1979**, *6*, 261.
(6) Dubler, E. *Met. Ions Biol. Syst.* **1996**, *Vol 32* (32), 301.
(7) Lippert, B. *Cisplatin*; Wiley-VCH: Weinheim, Germany, 1999.
(8) Kirschner, S.; Wei, Y. K.; Francis, D.; Bergman, J. G. *J. Med. Chem.* **1969**, *9*, 369.
(9) Das, M.; Livingstone, S. E. *Br. J. Cancer* **1978**, *38*, 325.
(10) Houlton, A. *Adv. Inorg. Chem.* **2002**, *53*, 87.
(11) Zamora, F.; Amo-Ochoa, P.; Sanz Miguel, P. J.; Castillo, O. *Inorg. Chim. Acta* **2009**, *362*, 691.
(12) Amo-Ochoa, P.; Castillo, O.; Alexandre, S. S.; Welte, L.; de Pablo, P. J.; Rodriguez-Tapiador, M. I.; Gomez-Herrero, J.; Zamora, F. *Inorg. Chem.* **2009**, *48*, 7931.
(13) Alexandre, S. S.; Soler, J. M.; Miguel, P. J. S.; Nunes, R. W.; Yndurain, F.; Gomez-Herrero, J.; Zamora, F. *Appl. Phys. Lett.* **2007**, *90*, 193107.
(14) Amo-Ochoa, P.; Rodriguez-Tapiador, M. I.; Castillo, O.; Olea, D.; Guijarro, A.; Alexandre, S. S.; Gomez-Herrero, J.; Zamora, F. *Inorg. Chem.* **2006**, *45*, 7642.
(15) Olea, D.; Alexandre, S. S.; Amo-Ochoa, P.; Guijarro, A.; de Jesus, F.; Soler, J. M.; de Pablo, P. J.; Zamora, F.; Gomez-Herrero, J. *Adv. Mater.* **2005**, *17*, 1761.
(16) Wettig, S. D.; Wood, D. O.; Aich, P.; Lee, J. S. *J. Inorg. Biochem.* **2005**, *99*, 2093.
(17) Alexandre, S. S.; Soler, J. M.; Seijo, L.; Zamora, F. *Phys. Rev. B* **2006**, *73*, 205112.
(18) Coronado, E.; Galan-Mascaros, J. R.; Gomez-Garcia, C. J.; Laukhin, V. *Nature* **2000**, *408*, 447.
(19) Ohno, H.; Chiba, D.; Matsukura, F.; Omiya, T.; Abe, E.; Dietl, T.; Ohno, Y.; Ohtani, K. *Nature* **2000**, *408*, 944.
(20) Nakamoto, K. *Infrared and Raman Spectra of Inorganic and Coordination Compounds*; John Wiley & Sons: Hoboken, NJ, 2009.
(21) Altomare, A.; Burla, M. C.; Camalli, M.; Cascarano, G. L.; Giacovazzo, C.; Guagliardi, A.; Moliterni, A. G. G.; Polidori, G.; Spagna, R. *J. Appl. Crystallogr.* **1999**, *32*, 115.
(22) Sheldrick, G. M. *Acta Crystallogr.* **2008**, *A64*, 112.
(23) Farrugia, L. J. *WINGX. A Windows Program for Crystal Structure Analysis*; University of Glasgow: Glasgow, 1998.
(24) Vandersluis, P.; Spek, A. L. *Acta Crystallogr., Sect. A* **1990**, *46*, 194.
(25) Spek, A. L. *PLATON, A Multipurpose Crystallographic Tool*; Utrecht University: Utrecht, Holland,1998.
(26) Ordejon, P.; Artacho, E.; Soler, J. M. *Phys. Rev. B* **1996**, *53*, 10441.
(27) Soler, J. M.; Artacho, E.; Gale, J. D.; Garcia, A.; Junquera, J.; Ordejon, P.; Sanchez-Portal, D. *J. Phys.: Condens. Matter* **2002**, *14*, 2745.
(28) Chakarova-Kack, S. D.; Schroder, E.; Lundqvist, B. I.; Langreth, D. C. *Phys. Rev. Lett.* **2006**, 96.
(29) Chakarova-Kack, S. D.; Vojvodic, A.; Kleis, J.; Hyldgaard, P.; Schroder, E. *New. J. Phys.* **2010**, 12.
(30) Roman-Perez, G.; Soler, J. M. *Phys. Rev. Lett.* **2009**, 103.
(31) Sankey, O. F.; Niklewski, D. J. *Phys. Rev. B* **1989**, *40*, 3979.
(32) Louie, S. G.; Froyen, S.; Cohen, M. L. *Phys. Rev. B* **1982**, *26*, 1738.
(33) Dubler, E.; Gyr, E. *Inorg. Chem.* **1988**, *27*, 1466.
(34) Janiak, C. *J. Chem. Soc., Dalton Trans.* **2000**, 3885.
(35) Benmansour, S.; Setifi, F.; Triki, S.; Gomez-Garcia, C. J. *Inorg. Chem.* **2012**, *51*, 2359.
(36) Podgajny, R.; Chorazy, S.; Nitek, W.; Budziak, A.; Rams, M.; Gomez-Garcia, C. J.; Oszajca, M.; Lasocha, W.; Sieklucka, B. *Cryst. Growth Des.* **2011**, *11*, 3866.
(37) Lloret, F.; Julve, M.; Cano, J.; Ruiz-Garcia, R.; Pardo, E. *Inorg. Chim. Acta* **2008**, *361*, 3432.

(38) Etter, M. C. *Acc. Chem. Res.* **1990**, *23*, 120.
(39) Etter, M. C.; MacDonald, J. C.; Bernstein, J. *Acta Crystallogr.* **1990**, *B46*, 256.
(40) Etter, M. C. *J. Phys. Chem.* **1991**, *95*, 4601.
(41) Janiak, C.; Scharmann, T. G.; Mason, S. A. *J. Am. Chem. Soc.* **2002**, *124*, 14010.
(42) Liu, Q.-Y.; Li, X. *CrystEngComm* **2005**, *7*, 87.
(43) Naskar, J. P.; Drew, M. G. B.; Hulme, A.; Tocher, D. A.; Datta, D. *CrystEngComm* **2005**, *7*, 67.
(44) Sun, Y. Q.; Zhang, J.; Ju, Z. F.; Yang, G. Y. *Aust. J. Chem.* **2005**, *58*, 572.
(45) Janiak, C.; Scharmann, T. G.; Günther, W.; Girgsdies, F.; Hemling, H.; Hinrichs, W.; Lentz, D. *Chem.—Eur. J.* **1996**, *1*, 637.
(46) Janiak, C.; Scharmann, T. G.; Brzezinka, K.-W.; Reich, P. *Chem. Ber.* **1995**, *128*, 323.
(47) Janiak, C.; Scharmann, T. G.; Hemling, H.; Lentz, D.; Pickardt, J. *Chem. Ber.* **1995**, *128*, 235.
(48) Zhuge, F.; Wu, B.; Liang, J.; Yang, J.; Liu, Y.; Jia, C.; Janiak, C.; Tang, N.; Yang, X.-J. *Inorg. Chem.* **2009**, *48*, 10249.
(49) Zhuge, F.; Wu, B.; Dong, L.; Yang, J.; Janiak, C.; Tang, N.; Yang, X.-J. *Aust. J. Chem.* **2010**, *63*, 1358.
(50) Banerjee, S.; Sen, S.; Chakraborty, J.; Butcher, R. J.; Gómez García, C. J.; Puchta, R.; Mitra, S. *Aust. J. Chem.* **2009**, *62*, 1614−1621.
(51) Yamanari, K.; Fukuda, I.; Kawamoto, T.; Kushi, Y.; Fuyuhiro, A.; Kubota, N.; Fukuo, T.; Arakawa, R. *Inorg. Chem.* **1998**, *37*, 5611.
(52) Yamanari, K.; Ito, R.; Yamamoto, S.; Konno, T.; Fuyuhiro, A.; Fujioka, K.; Arakawa, R. *Inorg. Chem.* **2002**, *41*, 6824.
(53) Amo-Ochoa, P.; Sanz Miguel, P. J.; Castillo, O.; Houlton, A.; Zamora, F. In *Metal Complex-DNA Interactions*; Hadjiliadis, N., Sletten, E., Eds.; Wiley: Chichester, U.K., 2009; p 95.
(54) Thomas-Gipson, J.; Beobide, G.; Castillo, O.; Cepeda, J.; Luque, A.; Perez-Yanez, S.; Aguayo, A. T.; Roman, P. *Cryst. Eng. Commun.* **2011**, *13*, 3301.